

SUBGRID MARCHING TETRAHEDRA (SUPPLEMENTAL MATERIAL)

Hossein Baktash, Mark Gillespie, Keenan Crane

1 TABLES

Tables in this section help illustrate the kind of spanning surfaces that are used for primal contouring within a single tetrahedron. Recall that the full set of possibilities is not finite: our procedure defines spanning surfaces for any number of intersection points along edges. Here we hence show tables up to a maximum number of intersections per edge, picking a number large enough to communicate the essential structures arising from each type of boundary curve.

As in the paper, we index edge coordinates via the scheme $\mathbf{e} := (e_{01}, e_{02}, e_{03}, e_{23}, e_{13}, e_{12})$. For each curve type, we enumerate all possible intersection patterns up to at most n intersections per edge, keeping only those that are distinct up to symmetries of the tetrahedron. For instance, in Figure 1 we show a single corner cut at one vertex (001110), skipping the cases corresponding to a single corner cut at the other three vertices.

1.1 Corner Cuts

Figure 1 shows all distinct configurations of corner cuts, up to four intersections per edge, resulting in some number of triangular disks at each corner. Since these triangles can be added at the corners of any other configuration without otherwise changing the topology of the spanning disks, we omit them from subsequent tables.

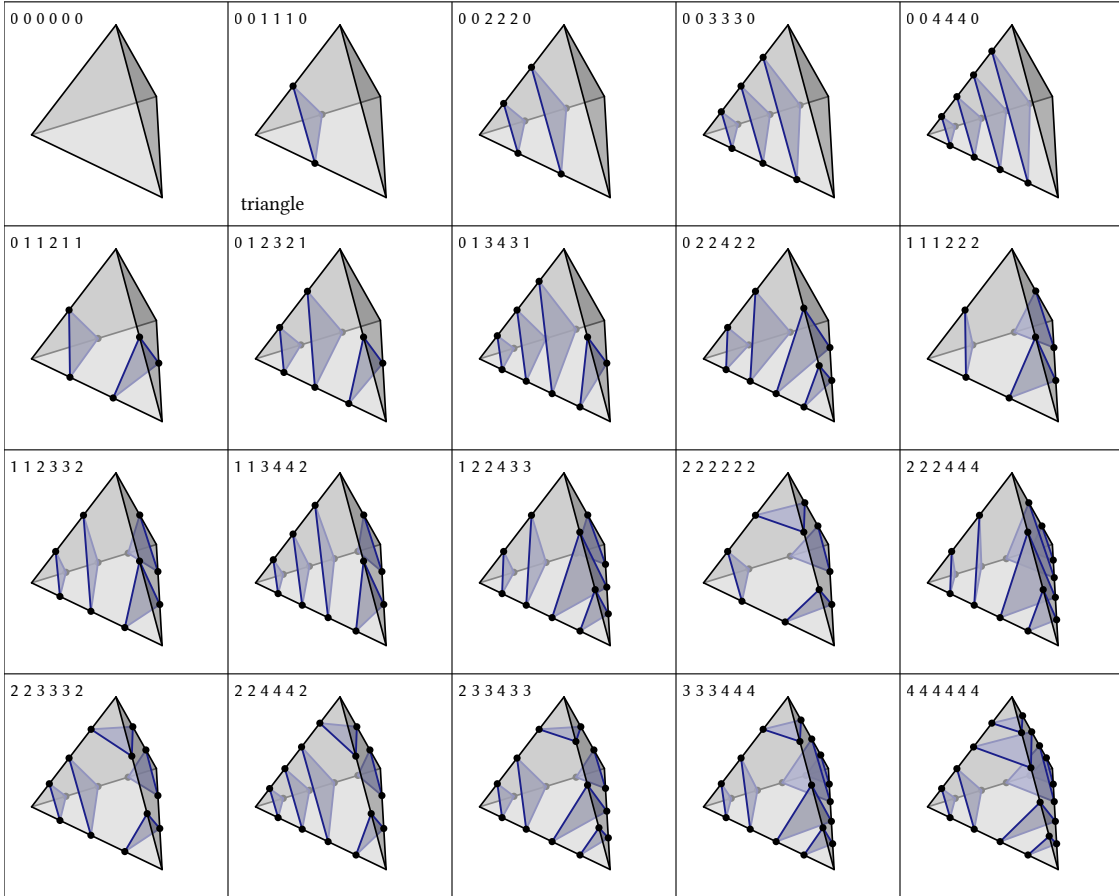


Fig. 1. **Corner cuts, up to four intersections per edge.** Corner cuts can be added to any other intersection pattern without changing the topology of the original spanning disks, and are hence omitted from subsequent tables.

1.2 Normal Boundary Curves

Figure 2 shows all configurations that yield only normal boundary curves (omitting those with corner cuts), up to six intersections per edge. Here we see several key cases, including quads, octagons, and other polygons whose number of sides is a multiple of four. The case of two dodecagons (246256) is the simplest configuration requiring subdivision and multiple Steiner points for a single polygon—such cases are rare until intersection counts become quite large. Notice that in all cases, $e_{01} = e_{23}$, $e_{02} = e_{13}$, and $e_{03} = e_{12}$.

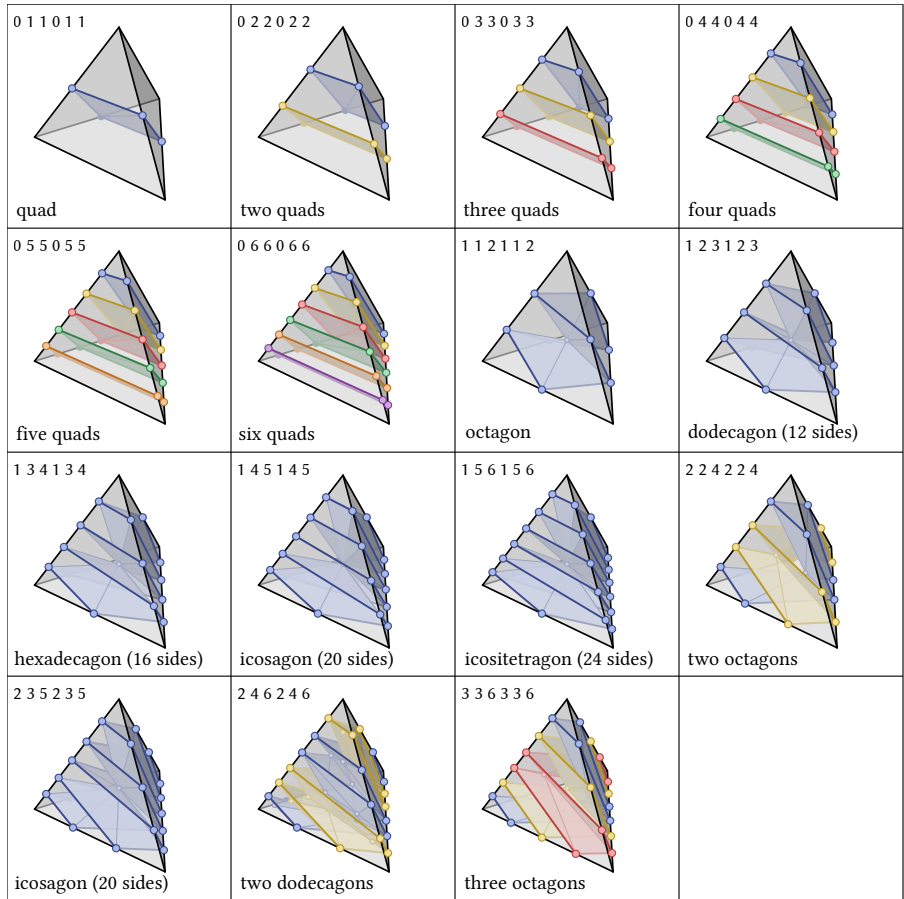


Fig. 2. **Normal boundary curves, up to six intersections per edge.** Quads and octagons provide some of our base cases, as do single polygons with many sides. The case of two dodecagons (246246) is the simplest configuration that requires subdivision and insertion of additional Steiner points, indicated by small open dots on the tet interior.

1.3 Non-normal Boundary Curves

Figure 3 shows all configurations that induce only non-normal boundary curves, up to four intersections per edge. Early on we see two basic types of polygons that can sit within a single tet face: quads (000022) and hexagons (000222). For larger intersection counts (e.g., 024224), we start to see polygonal strips that wind around the tet boundary—similar to spiraling normal boundary loops in Figure 2. Configurations 000022, 001112, and 011013 give examples of contractible, corner, and diagonal-type loops. Note that along some edges we have open segments, which do not form part of the output (but may belong to polygons produced by neighboring tets).

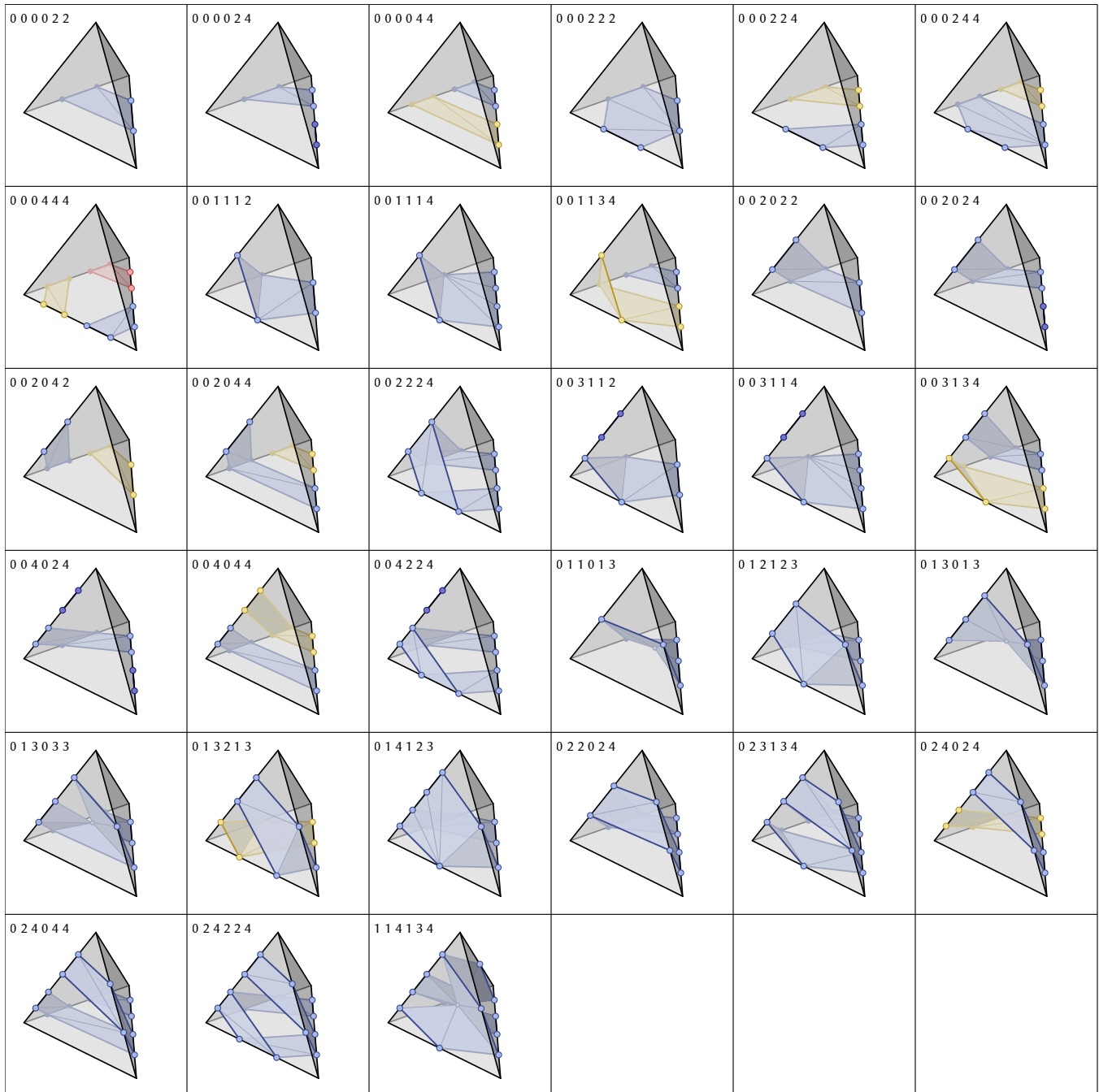


Fig. 3. **Non-normal boundary curves, up to four intersections per edge.** For visual simplicity, we omit additional Steiner points (interior to polygons) needed to produce a global embedding, rather than just a manifold Δ -complex.

1.4 All intersection patterns.

Finally, Figure 4 shows the reconstruction we obtain for all intersection patterns up to two intersections per edge. Here, several basic cases (highlighted in blue) quickly emerge: a contractible quad (000022), contractible hexagon (000222), corner cut triangle (001110), corner-type loop (001112), diagonal cut quad (011011), and octagon (112112). Here we also see that the full space of possibilities includes a large number of odd-sum configurations, which leave open boundaries (indicated by dashed lines) and unused points. However, these configurations will not arise from intersections sampled from a closed surface.

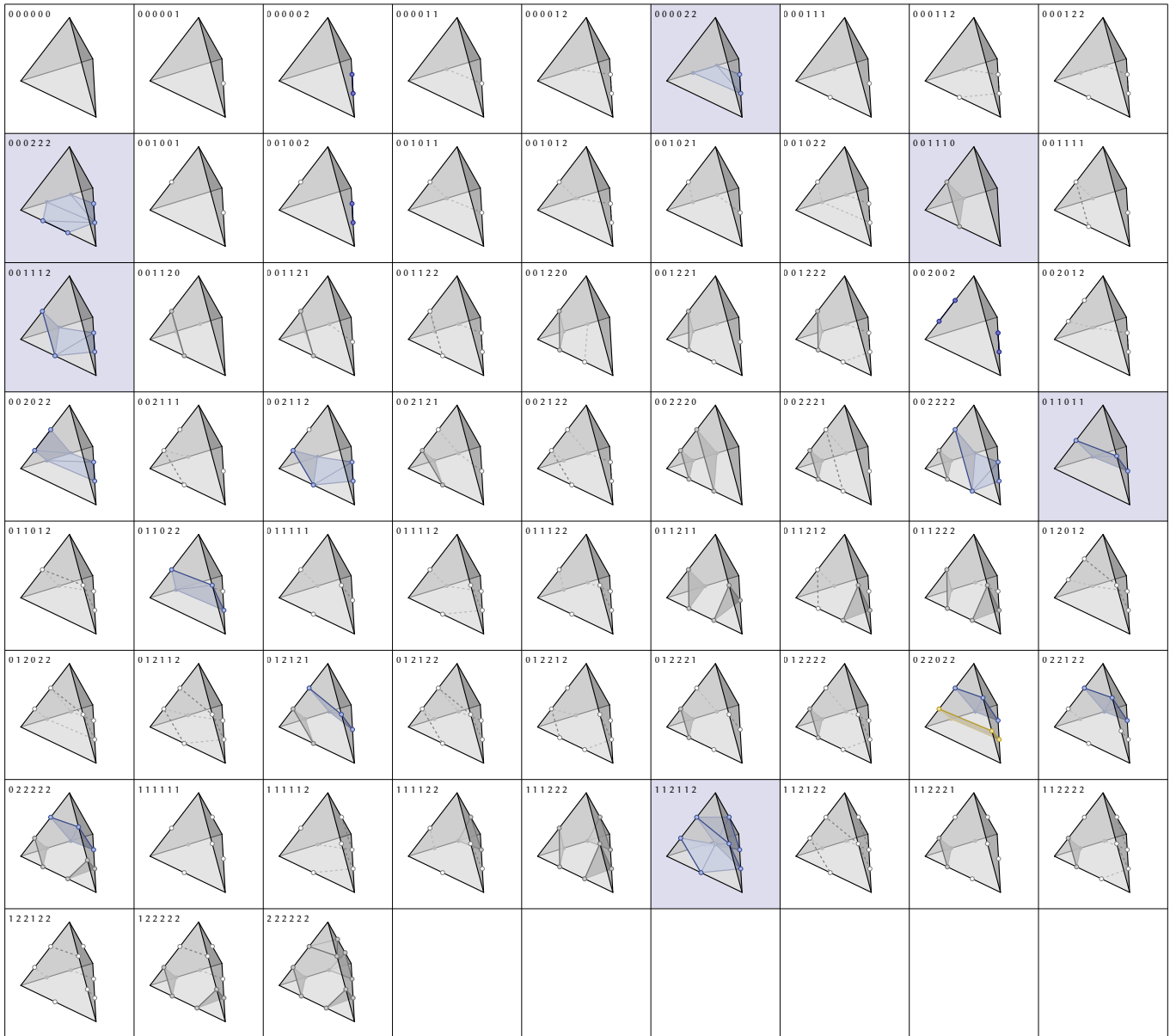


Fig. 4. All possible intersection patterns, up to two intersections per edge. Several basic cases are highlighted in blue. Dashed lines indicate open curves that are not part of the output for this tetrahedron (but may belong to closed curves from neighboring tetrahedra).

2 SCALING STATISTICS

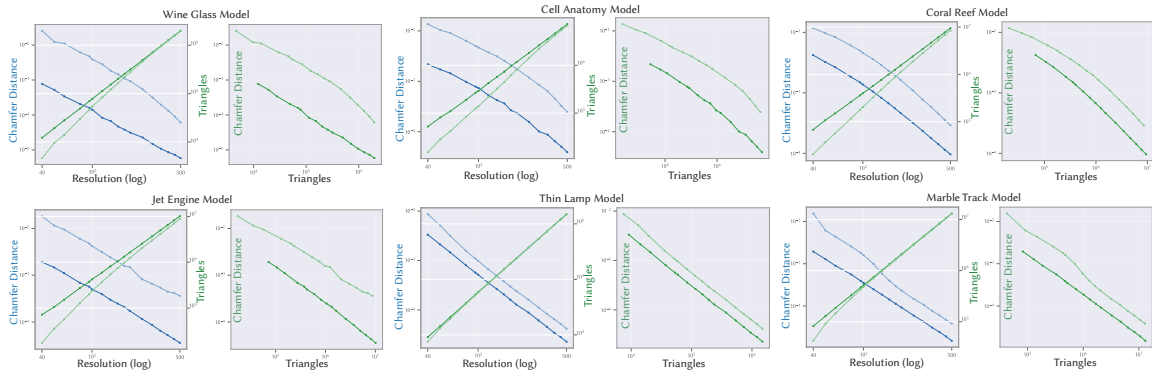


Fig. 5. Here we show statistics on the scaling of subgrid marching tets and classical marching tets on the triangle mesh examples shown in the main paper

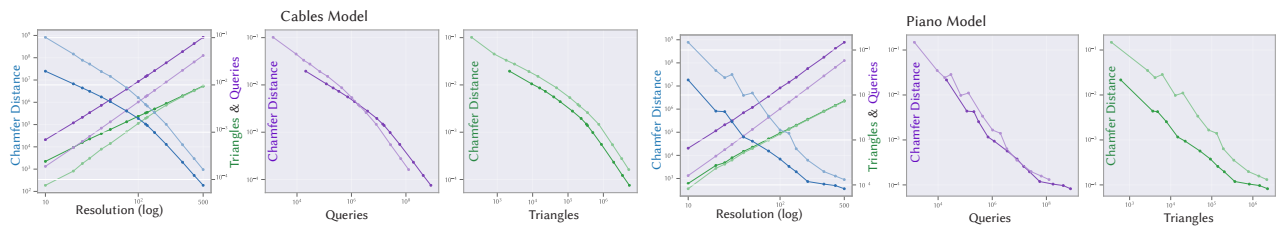


Fig. 6. Here we show statistics on the scaling of subgrid marching tets and classical marching tets on the SDF examples shown in the main paper